Supporting Information

Redox reactions of reduced flavin mononucleotide (FMN), riboflavin (RBF), and anthraquinone-2,6-disulfonate (AQDS) with ferrihydrite and lepidocrocite

Zhi Shi, John M. Zachara*, Liang Shi, Zheming Wang, Dean A. Moore, David W. Kennedy, Jim K. Fredrickson*

Pacific Northwest National Laboratory, PO Box 999, MS K8-96, Richland, WA 99352

Corresponding authors: Zhi Shi, phone: 1-509-371-6263, fax: 1-509-371-6354, e-mail: zshi4@jhu.edu; John M. Zachara, phone: 1-509-371-6355, fax: 1-509-371-6354, email: john.zachara@pnnl.gov.

August 2012

20 pages

---

6 Sections

3 Tables

9 Figures

Section S1. Water, Bottles, Anaerobic Glovebox, Chemicals and Reagents

Solutions were prepared from reagent grade chemicals and were used as received, unless otherwise stated. Distilled, deionized water (DDW) with a resistivity of 18 MΩ-cm (Barnstead nanopure) was used for all experiments. Bottles and glassware were soaked in 2 M hydrochloric acid (Sigma-Aldrich), rinsed with distilled water, soaked in 5 M nitric acid (Fisher Scientific), rinsed with distilled water, and then rinsed with DDW and air dried.

Reduced organic reductant preparation, redox reaction kinetic experiments, and sample analysis were conducted inside an anaerobic glovebox (100% N_2 atmosphere, Innovative Technology, Inc., Massachusetts) with PureLab GP 2-HE inert gas purifier with a packed copper catalyst and molecular sieve. The oxygen concentration inside the glovebox was below the detection limit (0.1 ppm) of the oxygen sensor. Deoxygenated, distilled, deionized water (DDDW) was prepared by boiling DDW in a 2 L bottle under vacuum for 2 hours, and then sparging with high purity nitrogen gas overnight in the glovebox. The dissolved oxygen concentration in the DDDW was occasionally checked using a colorimetric self-filling ampoule (CHEMetrics, Inc.), and the dissolved oxygen concentration was always below the detection limit (5 ppb).

Flavin mononucleotide (FMN), riboflavin (RBF), sodium dithionite (sodium hydrosulfite, technical grade, 85%), ferrozine reagent (3-(2-Pyridyl)-5,6-diphenyl-1,2,4-triazine-4′,4′′-disulfonic acid sodium salt), sodium acetate, $Fe(NO_3)_3{\cdot}9H_2O$, Na_2SiO_3, PIPES, and HEPES, were obtained from Sigma-Aldrich. Anthraquinone-2,6-disulfonate, disodium salt (AQDS) was obtained from Pfaltz & Bauer, Inc.

Section S2. Iron Oxides Synthesis and Characterization

2-Line ferrihydrite (2-line FH), 2-line Si-ferrihydrite (2-line Si-FH), 6-line ferrihydrite (6-line FH), and lepidocrocite (LEP) were synthesized according to methods of Schwertmann and Cornell (*1*) and Zachara et al. (*2*). Both 2-line FH and 2-line Si-FH were synthesized by hydrolysis of $Fe(NO_3)_3$ solution at pH 7 at room temperature. The syntheses were conducted inside an anaerobic glovebox to prevent CO_2 absorption. For 2-line FH, 140 grams of $Fe(NO_3)_3{\cdot}9H_2O$ was dissolved in 700 mL of DDDW in a 1000 mL Teflon bottle. The pH of the $Fe(NO_3)_3$ solution was slowly adjusted with 2.0 M NaOH solution to pH 7, yielding a dark brown suspension. The suspension was held at pH ~7 overnight. For 2-line Si-FH, 1.78 grams of Na_2SiO_3 was dissolved in 100 mL DDDW, and then added to $Fe(NO_3)_3$ solution before NaOH titration. The mole fraction of Si [i.e., Si/(Si+Fe)] was 0.0167. Si and Fe were co-precipitated during NaOH titration. Both suspensions were centrifuged and resuspended in DDW for 8 repetitions. The mole fraction of Si remained at 0.0167 after washing. Six-line FH was synthesized by hydrolysis of $Fe(NO_3)_3$ in 75 ˚C DDW with subsequent dialysis. Details of the synthesis and purification are provided elsewhere (*3*). Lepidocrocite was synthesized by air

oxidation of a $FeCl_2$ solution at pH 6.9 at room temperature, yielding a dark orange suspension (*1*). The lepidocrocite suspension was washed using the same procedure as used for the 2-line FH suspension.

The synthesized iron oxides were characterized using transmission electron microscopy (TEM), powder X-ray diffraction (XRD), and BET surface area analysis. Details of characterization methods are provided elsewhere (*2*). In brief, for TEM analysis, droplets of the diluted iron oxide suspension were dried onto 200 mesh holey carbon grids and examined by TEM (Jeol JEM 2010 TEM). The bright field TEM images are shown in Figure S1.

Subsamples of the iron oxide suspensions were rapidly frozen using liquid N_2 and then freeze-dried (Labconco freeze dry system, Kansas City, Missouri) for powder XRD and BET surface area analysis. Powder XRD patterns were acquired using a Philips PW 3040/00 X′pert MPD system, with CuKα radiation (λ = 0.15406 nm). A low-background quartz sample holder was used. The XRD patterns of 2-line FH and 2-line Si-FH were almost identical, with two very broad peaks at 36˚ and 63˚ (2θ Kα1) (Figure S2), and d-spacing values of 0.25 nm and 0.15 nm, consistent with reported values (*1*). The XRD pattern of 6-line FH displayed six broadened lines, in agreement with previous reports (*3*). The diffraction pattern of lepidocrocite matched the ICDD reference without detectable impurities (Figure S2).

BET surface areas were determined from nitrogen adsorption/desorption isotherms collected with a Quantachrome Autosorb 6-B gas sorption system. The freeze-dried iron oxides were degassed at 25˚C under vacuum and analyzed at 77.4 K. A five point BET method was used to calculate the surface area of each sample (Table S1). The measured BET surface areas were consistent with previously reported values (*1*).

Section S3. Preparation and Characterization of Reduced Forms of FMN, RBF, and AQDS

The reduced forms of FMN ($FMNH_2$) and RBF ($RBFH_2$) were prepared by dithionite reduction with subsequent purification inside an anaerobic glovebox. Approximately 0.5 gram of FMN was dissolved in 20 mL DDDW to yield a ~50 mM FMN solution. A small amount of sodium dithionite dry powder was gradually added to the FMN solution with continuous stirring. The dark red color of the FMN solution immediately changed to dark green with precipitation upon addition of dithionite. The dosage of dithionite was incrementally decreased during the reduction procedure to minimize residual, unreacted dithionite. The color further changed to blackish green, then to dark brown, and finally to vivid red-orange with precipitates. Only small amounts of sodium dithionite were added toward the end of the procedure to minimize residual dithionite. The final red-orange suspension was transferred to 2.0 mL centrifuge tubes, and centrifuged for 2 minutes at 13000 rpm. After discarding the supernatant, the precipitates were collected, resuspended in 1.0 mL acidic methanol solution (10% 3 mM HCl, 90% deoxygenated methanol, v:v), and centrifuged for 2 minutes at 13000 rpm. The washing procedure was repeated two more times to remove excess dithionite and other inorganic products. The washed

precipitates were dried inside the glovebox. The dried material was then dissolved in DDDW to yield a stock solution. The concentration of the $FMNH_2$ stock solution was determined by fully re-oxidizing an aliquot in air, and determining its concentration using UV-visible spectrophotometry with the extinction coefficient of FMN (Table 1 in the main text). UV-visible spectra of FMN and $FMNH_2$ are shown in Figure S3.

$RBFH_2$ was prepared using a similar method with slight modification. The aqueous solubility of RBF is below 50 mM at pH 7.0. Therefore, 20 μL of 5.0 M NaOH was added to elevate pH to the point where a 50 mM riboflavin solution could be obtained. During the washing procedure, the orange-yellow precipitates were washed with DDDW 3 times. Methanol was not needed because the aqueous solubility of $RBFH_2$ is low. The concentration of the $RBFH_2$ stock solution was determined using the re-oxidation method.

Bioreduced AH_2DS was prepared by incubation of AQDS with *Shewanella oneidensis* strain MR-1 and H_2 (electron donor) at pH 7.0 (PIEPS buffer). Details of the preparation method are described elsewhere (*2*).

The reductant stock solutions were kept in glass serum bottles sealed with thick rubber stoppers, wrapped in black aluminum foil (LEE filters, Burbank, CA) to prevent photo-degradation, and stored inside the glovebox at room temperature.

Section S4. Reducing Equivalents of the Synthesized Organic Reductants

$FMNH_2$, $RBFH_2$, and AH_2DS are all two-electron reductants (Table 1 in the main text). Fixed amounts of dissolved ferric oxidant, $Fe^{III}EDTA$ (100 μM), and a solid ferric oxidant, lepidocrocite (50 μM and 250 μM), were used to test the purity of the synthesized $FMNH_2$, $RBFH_2$, and AH_2DS stock solutions. The $FMNH_2$, $RBFH_2$, and AH_2DS solutions were used at nominal concentrations of 10, 20, 30, 40, and 50 μM. The organic species and Fe^{II}_{aq} concentrations were measured immediately after redox reaction. We expected to see less than two mole equivalents of ferrous iron generated if $FMNH_2$, $RBFH_2$, or AH_2DS were not in their fully reduced forms. Alternatively, we expected to see more than two mole equivalents of ferrous iron generated per mole of oxidized reductant, if there were some residual dithionite and sulfite anions that had not been completely removed during washing procedure.

The test experiments verified that the $FMNH_2$, $RBFH_2$, and AH_2DS stock solutions were fully reduced without residual dithionite or sulfite (Figure S4). Exactly two mole equivalents of Fe^{II} were generated for each mole of oxidized reductant. The $FMNH_2$, $RBFH_2$, and AH_2DS stock solutions were tested occasionally during the experimental campaign using the above method, and they were stable for at least 3 months inside the anaerobic glovebox in dark.

Section S5. Redox Experimental Design and Data Analysis

Batch and stopped flow redox experiments were conducted to study reaction stoichiometry and kinetics. Both organic species and ferrous iron were analyzed as a function a time in the batch experiments, enabling quantification of reaction stoichiometry and rate. The rapid reaction kinetics limited the conditions under which useful batch experiments could be performed. The stopped-flow methodology was much more suitable to the rapid reaction rates found for this system. It was consequently applied to study solids concentration and pH effects on the reductive dissolution reaction. However, ferrous iron analyses are not easily integrated into the stopped-flow methodology and these were consequently not performed.

Batch Experiment and Data Analysis

Batch experiments were conducted in 125 mL polypropylene bottles that were stirred with Teflon-coated stir bars inside the anaerobic glovebox. The reaction bottles were wrapped with black aluminum foil for the duration of the experiment in order to prevent photo-degradation of the organic reactant or product. The temperature of the glovebox atmosphere was held at 21 ± 0.5 ˚C for the duration of the kinetic experiments. The pH of the reaction solution/suspension was maintained at pH 7.0 using 30 mM PIPES buffer. pH values were measured before and after reaction (Orion pH meter and semimicro pH probe, Orion pH standards) to verify pH stability. Variations in pH were less than ±0.03 pH. A constant ionic strength was maintained by the 30 mM PIPES buffer without the addition of any other electrolytes.

Calculated volumes of DDDW, PIPES buffer, and iron oxide stock suspension were added to 125 mL polypropylene bottles (total reactant volume: 100 mL) and stirred for one hour to reach surface equilibrium. After that, 0.5 mL of organic reductant stock solution was added to initiate the redox reaction. A typical batch experiment contained 50 μM iron oxide and 20 μM organic reductant. Suspension aliquots (5.0 mL) were collected at 0.5, 1, 1.5, 2, 3, 5, 10, 20, 30, and 60 minutes, and immediately filtered through 0.2 μm Nylon syringe filter membranes (Whatman). The redox reaction was quenched by filtration. Aqueous organic product concentrations were immediately measured by UV-Vis spectrophotometry (HP8452 diode array, Agilent) inside the glovebox using quartz cuvettes. Fe^{II}(aq) was measured by ferrozine assay. Fe^{II}(aq) concentrations were calculated using the known extinction coefficient of the Fe^{II}-ferrozine complex ($\varepsilon = 27900\ M^{-1}\cdot cm^{-1}$ at 562 nm wavelength, *8*). Calculated values were in agreement with Fe^{II}(aq) standard calibration results. Total dissolved Fe was measured by ICP-OES (Perkin Elmer) for select samples.

A second-order kinetic model was used to fit the time course data. The second-order kinetic model can be described as follows using lepidocrocite as an example.

$$H_2X + 2Fe^{III}OOH(s, LEP) + 4H^+ = X + 2Fe^{2+} + 4H_2O \quad (S1)$$

where H_2X represents the organic reductant and X represents the oxidized product. The initial conditions are: $[H_2X]_o = 20\ \mu M$, $[FeOOH]_o = 50\ \mu M$, $[X]_o = [Fe^{2+}]_o = 0\ \mu M$, and subscript "$_o$" means initial condition at time zero. The following equations derive from the stoichiometry of reaction (S1):

$$[H_2X] = [H_2X]_o - [X] = [H_2X]_o - \frac{1}{2}[Fe^{2+}] \quad (S2)$$

$$[FeOOH] = [FeOOH]_o - 2[X] = [FeOOH]_o - [Fe^{2+}] \quad (S3)$$

It was assumed that the reaction rate (r) is first-order with respect to reductant concentration $[H_2X]$, oxidant concentration [FeOOH], and n^{th} order with respect to $[H^+]$. Measurements of pH revealed that $[H^+]$ was constant within any given experiment:

$$r = \frac{d[X]}{dt} = \frac{d[Fe^{2+}]}{2dt} = k'[H_2X][FeOOH][H^+]^n = k[H_2X][FeOOH] \quad (S4)$$

Where k' is the $(n+2)^{th}$-order reaction rate constant, and k is the second-order reaction rate constant, $k = k'[H^+]^n$.

Substitution of equations (S2) and (S3) in equation (S4) yields:

$$r = \frac{d[X]}{dt} = k\{[H_2X]_o - [X]\}\{[FeOOH]_o - 2[X]\} \quad (S5)$$

$$r = \frac{d[Fe^{2+}]}{2dt} = k\left\{[H_2X]_o - \frac{1}{2}[Fe^{2+}]\right\}\{[FeOOH]_o - [Fe^{2+}]\} \quad (S6)$$

Solving equations (S5) and (S6) by the partial fraction method provides a solution for [X] and $[Fe^{2+}]$:

$$[X] = \frac{\frac{1}{2}[FeOOH]_o[H_2X]_o(e^{[FeOOH]_o kt} - e^{2[H_2X]_o kt})}{\frac{1}{2}[FeOOH]_o e^{[FeOOH]_o kt} - [H_2X]_o e^{2[H_2X]_o kt}} \quad (S7)$$

$$[Fe^{2+}] = 2[Z] = \frac{[FeOOH]_o[H_2X]_o(e^{[FeOOH]_o kt} - e^{2[H_2X]_o kt})}{\frac{1}{2}[FeOOH]_o e^{[FeOOH]_o kt} - [H_2X]_o e^{2[H_2X]_o kt}} \quad (S8)$$

The second-order reaction rate constant k ($M^{-1}\cdot s^{-1}$) is the only unknown parameter in these equations. The kinetic model for ferrihydrite can be derived using the same method. Values of k were obtained by fitting the experimental data with Global Curve Fit Wizard in SigmaPlot version 11.0 (Systat Software, Inc.).

Stopped-Flow Experiment and Data Analysis

The rapid initial reaction stage was studied using a stopped-flow apparatus (BioLogic SF-4). The experiments were performed inside an anaerobic glovebox with reductant or product monitoring by a BioLogic MOS-250 spectrometer. The organic reactant stock solution and iron

oxide stock suspension were diluted to concentrations that were twice the initial desired reaction condition in two 50 mL tubes with pH buffer (i.e., for reaction with 50 μM $FMNH_2$ and 100 μM lepidocrocite, 100 μM $FMNH_2$ and 200 μM lepidocrocite were prepared in appropriate pH buffer). The iron oxide suspension was equilibrated in the buffer for 1 hour to achieve surface equilibration, and well-shaken before transfer to the stopped-flow system. These two reactant solutions were transferred to two 10 mL plastic syringes, and loaded to the stopped-flow system. The kinetic measurement was performed immediately to minimize the potential effect of particle settling inside the stopped-flow apparatus. Each experiment (i.e., shot) involved the mixing of 101 μL of reductant and 101 μL of oxidant at a flow rate of 14.00 $mL \cdot s^{-1}$. An increase in absorbance at 450 nm ($\lambda_{max, FMN}$ and $\lambda_{max, RBF}$) was measured for reactions with $FMNH_2$ and $RBFH_2$, which allowed the calculation of FMN or RBF production with time after proper baseline correction. For reactions with AH_2DS, a decrease in absorbance at 386 nm ($\lambda_{max, AH2DS}$) was measured for the oxidation of AH_2DS. The stopped-flow syringe systems were washed with DDDW 10 times after each run to avoid cross contamination.

The concentration of the oxidized organic reductant was calculated using the following procedure. The redox reaction between $FMNH_2$ and lepidocrocite (reaction (S9)) serves as an example.

$$FMNH_2 + 2Fe^{III}OOH(s, LEP) + 4H^+ = FMN + 2Fe^{2+} + 4H_2O \quad (S9)$$

The total absorbance measured at 450 nm (A_t) is the sum of the absorbance of FMN, $FMNH_2$, and the remaining lepidocrocite particles due to their light scattering/absorbance effect.

$$A_t = [FMN]\varepsilon_{FMN} + [FMNH_2]\varepsilon_{FMNH_2} + [FeOOH]\varepsilon_{FeOOH} \quad (S10)$$

$$[FMNH_2]_o = [FMN] + [FMNH_2] \quad (S11)$$

$$[FeOOH] = [FeOOH]_o - 2[FMN] \quad (S12)$$

where [FMN], $[FMNH_2]$, and [FeOOH] are concentrations of FMN, $FMNH_2$, and lepidocrocite at any given time, and $[FMNH_2]_o$ and $[FeOOH]_o$ are the initial $FMNH_2$ and lepidocrocite concentrations at time zero. The extinction coefficients of FMN, $FMNH_2$, and lepidocrocite at 450 nm are ε_{FMN}, ε_{FMNH2}, and ε_{FeOOH}. Solving equations S10 to S12 yields [FMN]:

$$[FMN] = \frac{A_t - [FMNH_2]_o\varepsilon_{FMNH_2} - [FeOOH]_o\varepsilon_{FeOOH}}{\varepsilon_{FMN} - \varepsilon_{FMNH_2} - 2\varepsilon_{FeOOH}} \quad (S13)$$

The concentrations of RBF and AH_2DS were calculated with a similar procedure.

Section S6. Adsorption of FMN and RBF onto Fe(III) oxides

Adsorption of 50 μM FMN or 50 μM RBF onto 30 mM 2-line ferrihydrite, 2-line Si-ferrihydrite, or lepidocrocite was performed at pH 7.0 in 30 mM PIPES buffer in dark. Because the reduced forms of flavins ($FMNH_2$ or $RBFH_2$) instantly reacted with Fe(III) oxides, only adsorption of oxidized forms of flavins was studied. The adsorption experiment was conducted in 15 mL polypropylene centrifuge tubes, and the Fe(III) oxide was continuously agitated using a vertical rotator for 24 hours. Fe(III) oxide was removed by filtration (0.2 μm Nylon syringe filter), and aqueous FMN or RBF concentration in the filtered solution was immediately measured by UV-Vis. Adsorbed FMN or RBF concentration was calculated from the difference between total added concentration and aqueous concentration (Figure S8). Desorprtion experiment confirmed that irreversible degradation was not taking place under these experimental conditions. It should be noticed that Fe(III) oxide concentration was 300 times higher than that in our redox experiment, in order to discern adsorption.

References:

(1) Schwertmann, U.; Cornell, R. M. *Iron Oxides in the Laboratory: Preparation and Characterization*; Wiley-VCH: Weinheim, 2000; pp.93-95, pp.104-105.

(2) Zachara, J. M.; Kukkadapu, R. K.; Peretyazhko, T.; Bowden, M.; Wang, C. M.; Kennedy, D. W.; Moore, D.A.; Arey, B. The mineralogic transformation of ferrihydrite induced by heterogeneous reaction with bioreduced anthraquinone disulfonate (AQDS) and the role of phosphate. *Geochim. Cosmochim. Acta* **2011**, *75*, 6330-6349.

(3) Peretyazhko, T. S.; Zachara, J. M.; Kennedy, D. W.; Fredrickson, J. K.; Arey, B. W.; McKinley, J. P.; Wang, C. M.; Dohnalkova, A. C.; Xia, Y. Ferrous phosphate surface precipitates resulting from the reduction of intragrain 6-line ferrihydrite by Shewanella oneidensis MR-1. *Geochim. Cosmochim. Acta* **2010**, *74*, 3751-3767.

(4) Cornell, R. M.; Schwertmann, U. *The Iron Oxides: Structure, Properties, Reactions, Occurrences, and Uses*; Wiley: Weinheim, 2003.

(5) Stumm, W.; Morgan, J. J. *Aquatic chemistry: chemical equilibria and rates in natural waters*; Wiley-Interscience: New York, 1996.

(6) Robie, R. A.; Hemingway, B. S.; Fisher, J. R. *Thermodynamic properties of minerals and related substances at 298.15 K and 1 Bar (105 Pascals) pressure and at high temperatures; U.S. Geological Survey Bulletin 1452*; United States Government Printing Office: Washington, 1978.

(7) van Schuylenborgh J. Sesquioxide formation and transformation. In: Schlichting, E. and Schwertmann U. (eds) Pseudogley and gley. Trans. Comm. V & VI Int. Soil Sci. Soc., VCH, Weinheim, 1973; p. 91-102.

(8) Stookey, L. L. Ferrozine - a new spectrophotometric reagent for iron. *Anal. Chem.* **1970**, *42*, 779-781.

Table S1. Relevant properties of iron oxides synthesized in this study.

Iron oxides	One-electron half reaction (relevant ΔG_f^o and ΔG^o values are provided under each species or half reaction)	Reduction potentials [a] (mV)		BET surface area ($m^2 \cdot g^{-1}$)	Surface area loading [b] ($m^2 \cdot L^{-1}$)	pH_{zpc} [c]
		E^o	E'			
Ferrihydrite (FH)	$Fe(OH)_3(s) + 3H^+ + e^- = Fe^{2+} + 3H_2O$ -699[d] $kJ \cdot mole^{-1}$ -78.87[e] -237.1[e] $\Delta G^o = -91.17\ kJ \cdot mole^{-1}$	945	60	230 (2-line FH) 280 (2-line Si-FH) 280 (6-line FH)	2.46 (2-line FH) 2.99 (2-line Si-FH) 2.99 (6-line FH)	7.8-7.9
Lepidocrocite (LEP)	γ-$FeOOH(s) + 3H^+ + e^- = Fe^{2+} + 2H_2O$ -477.7[f] $kJ \cdot mole^{-1}$ -78.87[e] -237.1[e] $\Delta G^o = -75.37\ kJ \cdot mole^{-1}$	781	-104	130	1.15	6.7-7.5

[a] Calculated using $E^o = -\Delta G^o/nF$, and Nernst equation. E': pH 7.0, 1 μM total dissolved iron.

[b] Surface area loading for a typical 100 μM Fe(III) oxide suspension. Surface area loading ($m^2 \cdot L^{-1}$) = molar concentration ($moles \cdot L^{-1}$) × molecular weight ($g \cdot mole^{-1}$) × surface area ($m^2 \cdot g^{-1}$).

[c] Reference (*4*). [d] Reference (*5*). [e] Reference (*6*). [f] Reference (*7*).

Table S2. Second-order kinetic model fitting parameters for batch reactions. Reaction conditions: 20 μM $FMNH_2$ or $RBFH_2$, 50 μM 2-line ferrihydrite (FH) or lepidocrocite (LEP), pH 7.0 (30 mM PIPES buffer). For reaction (iii) and (iv), ± represents one stand deviation from duplicate reactions.

Reactions	$Flavin_{aq}$		Fe^{II}_{aq}	
	k ($M^{-1}\cdot s^{-1}$)	R^2	k ($M^{-1}\cdot s^{-1}$)	R^2
(i) 2-line FH + $FMNH_2$	85	0.994	90	0.994
(ii) 2-line FH + $RBFH_2$	83	0.981	90	0.989
(iii) LEP + $FMNH_2$	537 ± 71	0.926, 0.931	463 ± 28	0.980, 0.977
(iv) LEP + $RBFH_2$	234 ± 11	0.991, 0.989	238 ± 36	0.997, 0.994

Table S3. Initial rate (r_o, $\mu M \cdot s^{-1}$) and surface area normalized initial rate (r_a, $\mu moles \cdot m^{-2} \cdot s^{-1}$) for redox reaction at various initial conditions. ± represents one stand deviation from at least 3 replicate experiments. "-": not measured due to limited aqueous solubility.

Reactions	Initial rate r_o ($\mu M \cdot s^{-1}$)					Initial rate r_a ($\mu moles \cdot m^{-2} \cdot s^{-1}$)				
	pH 4.0	pH 5.0	pH 6.1	pH 7.0	pH 8.0	pH 4.0	pH 5.0	pH 6.1	pH 7.0	pH 8.0
2-line FH with reductant										
$FMNH_2$	190 ± 2	116 ± 0.4	23 ± 0.1	8.3 ± 0.7	3.0 ± 0.1	77 ± 0.8	47 ± 0.2	9.5 ± 0.05	3.4 ± 0.3	1.2 ± 0.05
$RBFH_2$	-	-	-	12 ± 1.8	2.7 ± 0.3	-	-	-	4.9 ± 0.7	1.1 ± 0.1
AH_2DS	68 ± 1.6	56 ± 0.8	22 ± 0.3	9.5 ± 0.7	2.8 ± 0.1	28 ± 0.7	23 ± 0.3	8.8 ± 0.1	3.9 ± 0.3	1.1 ± 0.04
2-line Si-FH with reductant										
$FMNH_2$	79 ± 0.6	53 ± 0.2	15 ± 0.06	10.1 ± 0.9	4.4 ± 0.01	26 ± 0.2	18 ± 0.07	4.9 ± 0.02	3.4 ± 0.3	1.5 ± 0.01
$RBFH_2$	-	-	-	12 ± 1.5	4.4 ± 0.3	-	-	-	4.0 ± 0.5	1.5 ± 0.1
AH_2DS	41 ± 1.6	36 ± 0.3	21 ± 0.9	7.7 ± 0.9	4.6 ± 1.0	14 ± 0.5	12 ± 0.1	7.1 ± 0.3	2.6 ± 0.3	1.5 ± 0.3
6-line FH with reductant										
$FMNH_2$	32 ± 0.2	13 ± 0.3	7.4 ± 0.02	2.8 ± 0.2	0.31 ± 0.01	11 ± 0.06	4.3 ± 0.1	2.5 ± 0.01	0.94 ± 0.07	0.10 ± 0.01
$RBFH_2$	-	-	-	2.7 ± 0.03	0.50 ± 0.02	-	-	-	0.91 ± 0.01	0.17 ± 0.01
AH_2DS	18 ± 0.2	13 ± 0.1	7.0 ± 0.1	3.1 ± 0.03	0.54 ± 0.01	5.9 ± 0.06	4.4 ± 0.04	2.4 ± 0.02	1.0 ± 0.01	0.18 ± 0.01
Lepidocrocite with reductant										
$FMNH_2$	2.6 ± 0.006	1.9 ± 0.01	1.2 ± 0.01	1.3 ± 0.2	0.13 ± 0.01	2.3 ± 0.01	1.6 ± 0.01	1.1 ± 0.01	1.1 ± 0.2	0.11 ± 0.01
$RBFH_2$	-	-	-	0.67 ± 0.04	0.12 ± 0.03	-	-	-	0.58 ± 0.04	0.10 ± 0.03
AH_2DS	0.66 ± 0.01	0.42 ± 0.01	0.18 ± 0.01	0.14 ± 0.01	0.09 ± 0.01	0.58 ± 0.01	0.36 ± 0.01	0.16 ± 0.01	0.12 ± 0.01	0.08 ± 0.01

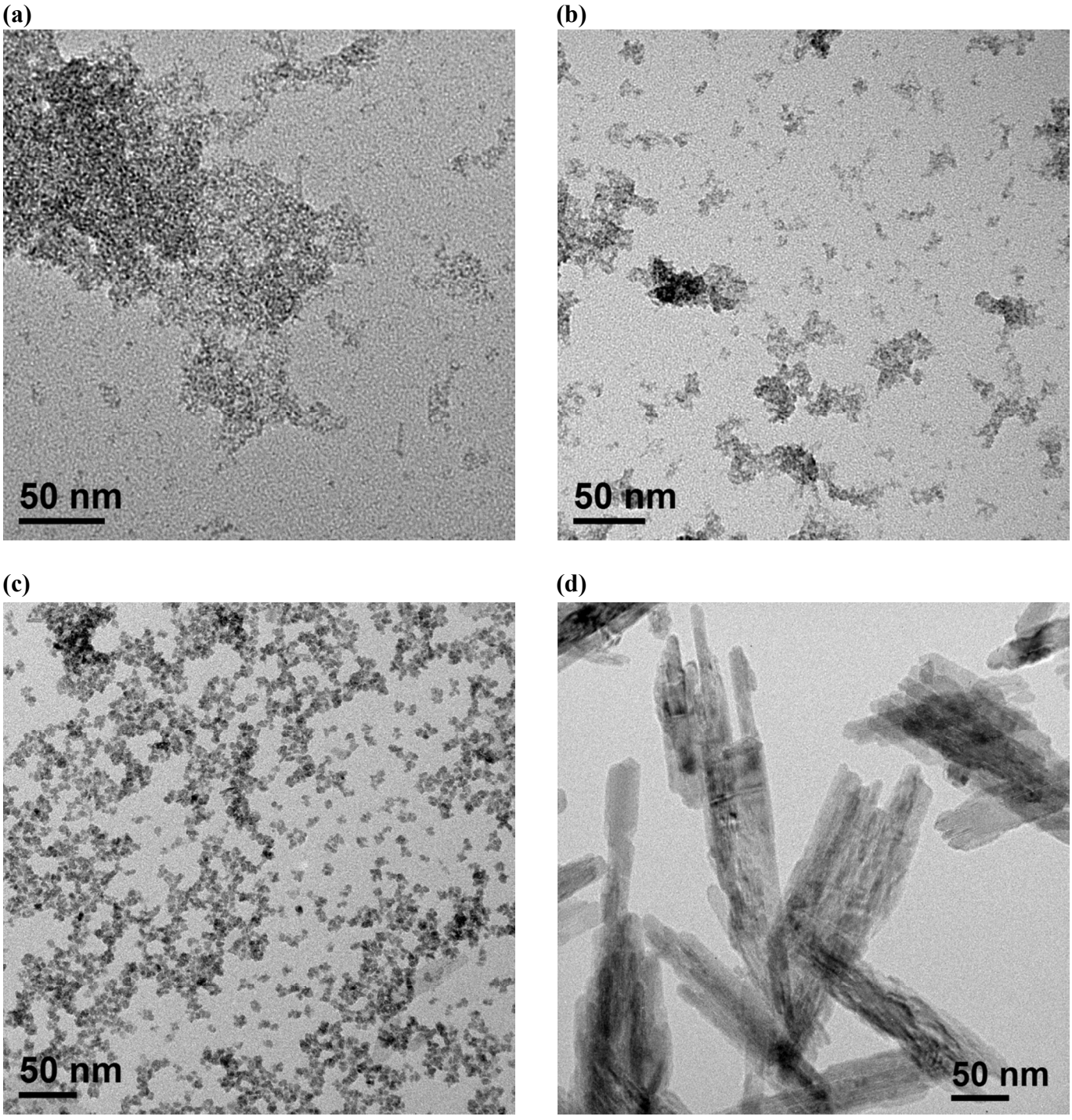

Figure S1. TEM images of four synthesized iron oxides. (a) 2-line FH, (b) 2-line Si-FH, (c) 6-line FH, and (d) lepidocrocite.

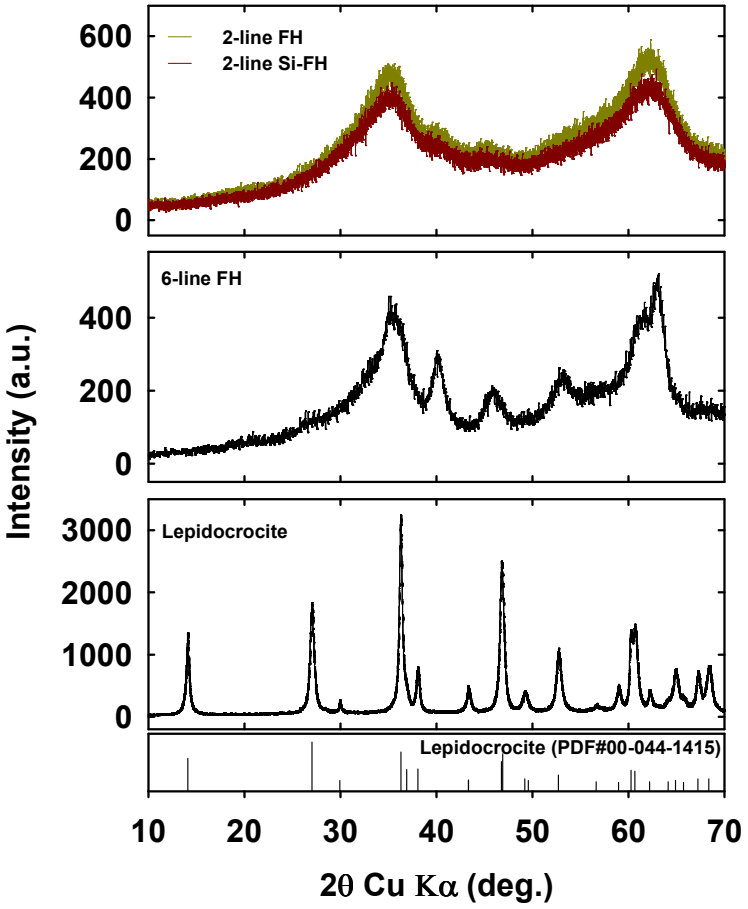

Figure S2. XRD patterns of four synthesized iron oxides: 2-line FH, 2-line Si-FH, 6-line FH, and lepidocrocite.

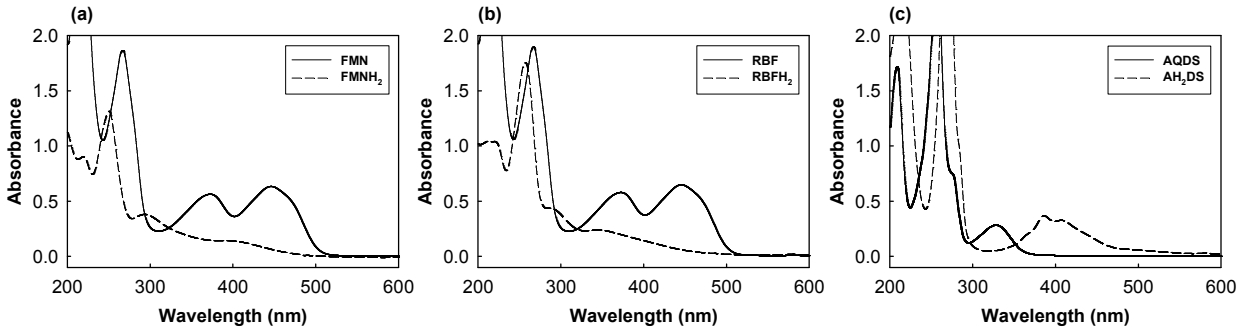

Figure S3. UV-Vis spectra of (a) FMN, $FMNH_2$; (b) RBF, $RBFH_2$; and (c) AQDS, AH_2DS redox couples. Each spectrum was acquired using 50 μM oxidized species from authentic standard reagent (solid line) or 50 μM reduced species solution made from synthesized stock solution (dash line) at pH 7.0 (30 mM HEPES).

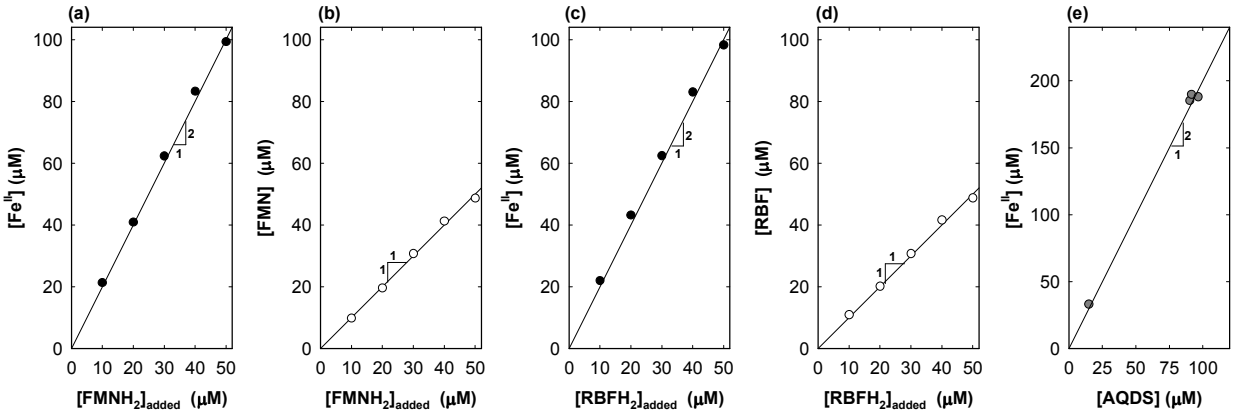

Figure S4. Reducing equivalents of synthesized reductants. (a) and (b): $FMNH_2$; (c) and (d): $RBFH_2$; (e) AH_2DS. $FMNH_2$ and $RBFH_2$ were fully oxidized by 100 μM $Fe^{III}EDTA$ at pH 3.0 (adjusted using 2.0 M HCl solution); AH_2DS was oxidized by lepidocrocite at pH 3.0 (adjusted using 2.0 M HCl solution). The slope of each straight line was labeled in the figure.

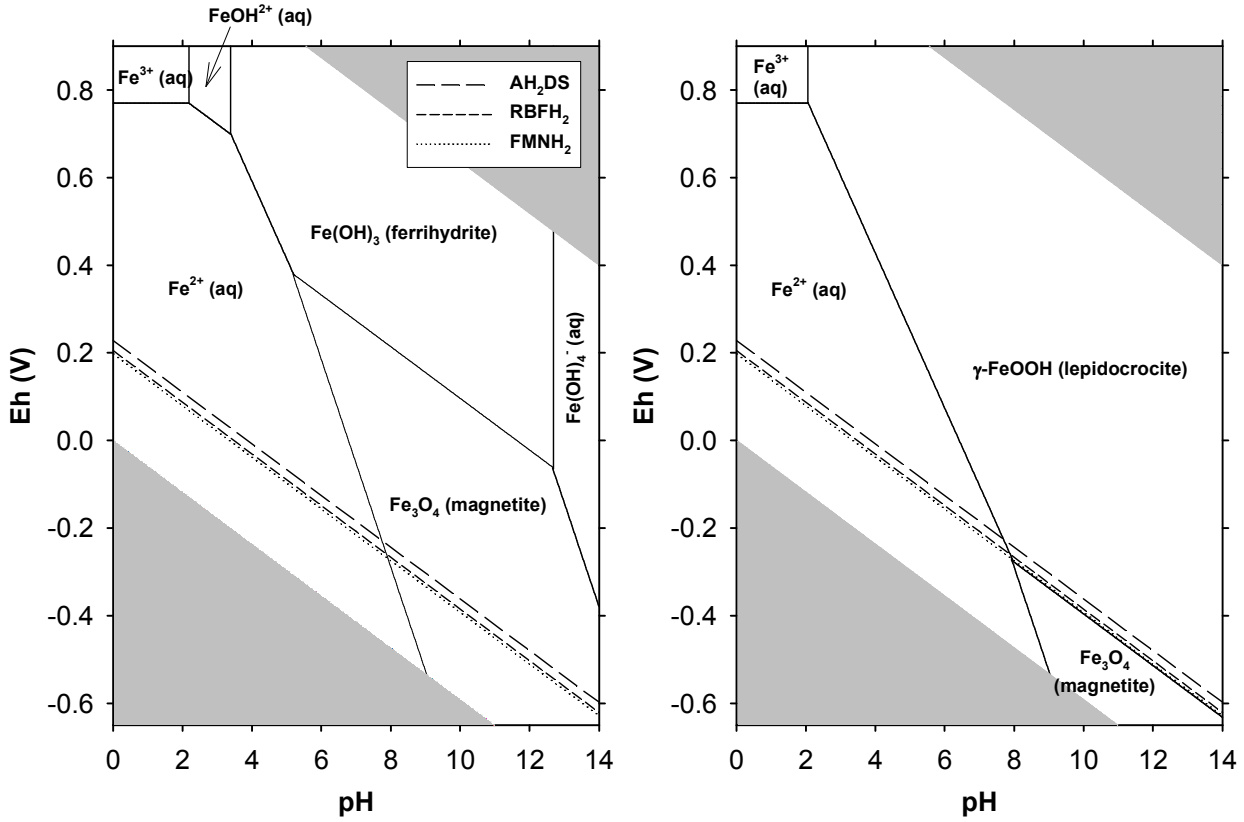

Figure S5. Eh-pH diagrams of ferrihydrite (left) and lepidocrocite (right) overlapped with Eh-pH curves for the $FMNH_2$/FMN, $RBFH_2$/RBF, and AH_2DS/AQDS redox couples. The white area is the stability region of water. Ferrihydrite and lepidocrocite diagrams were created using the Act2 program of the Geochemist's Workbench Professional 9.0 (Aqueous Solutions, LLC) and SigmaPlot. 1 μM total dissolved Fe was used for the calculation. Plotted lines for the organic reductants represent mid-point potentials.

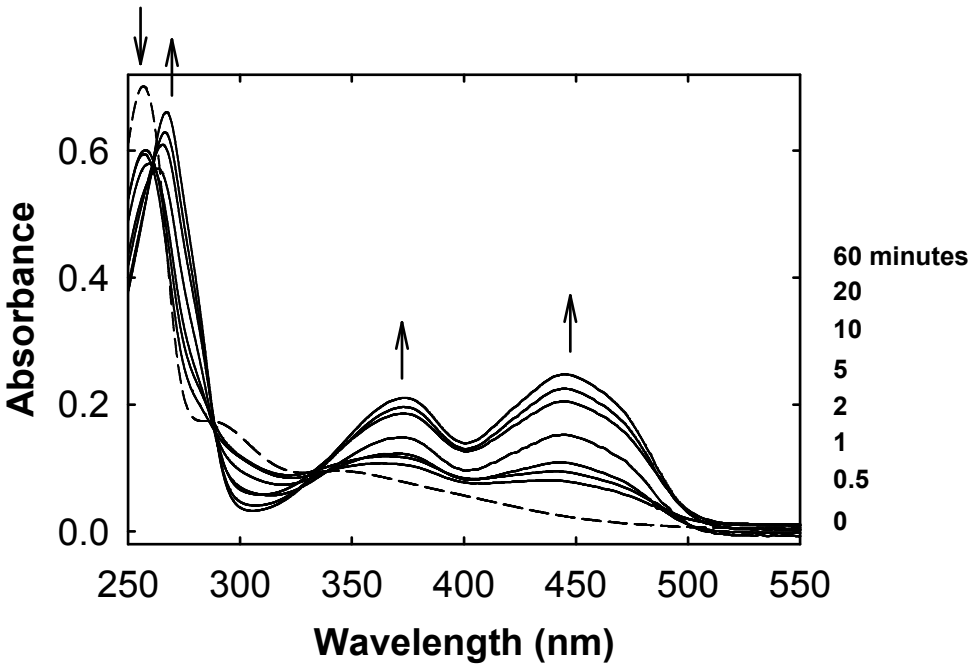

Figure S6. UV-Visible spectra of filtered reaction solution collected at 0.5, 1, 2, 5, 10, 20, and 60 minutes during oxidation of 20 μM $RBFH_2$ by 50 μM 2-line FH at pH 7.0 (30 mM PIPES buffer). Dashed line represents a pure 20 μM $RBFH_2$ standard solution (i.e., reaction time = 0). Upward or downward arrows indicate peak growth or decay as the reaction progresses.

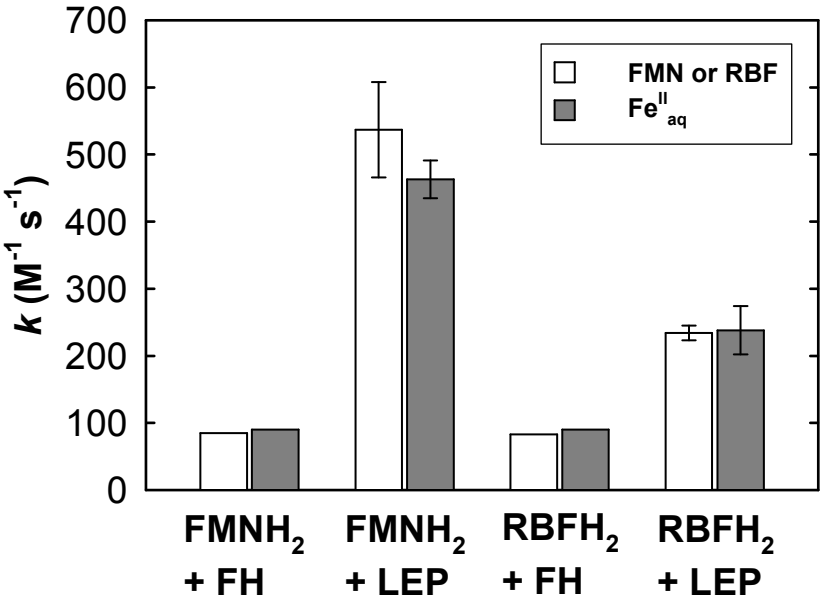

Figure S7. Second-order reaction rate constants (k) derived from the time course data in Figure 1 in the main text. Error bars represent one standard deviation from duplicate experiments.

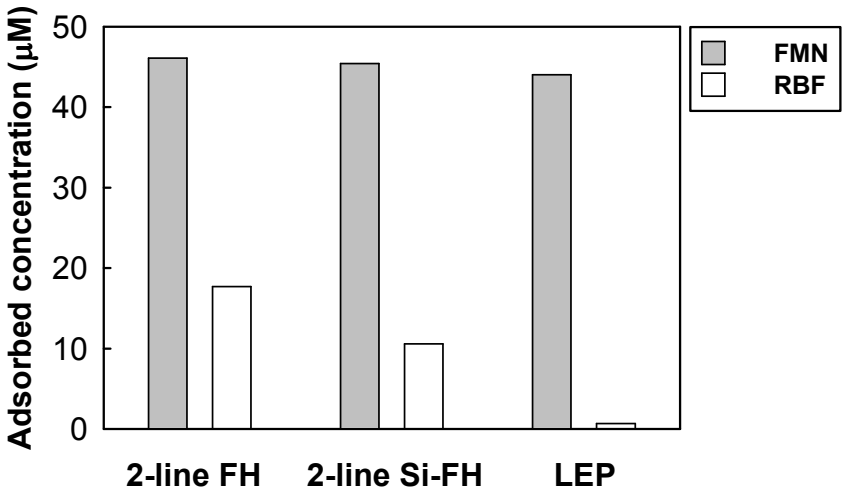

Figure S8. Adsorption of FMN or RBF onto 2-line ferrihydrite (FH), 2-line Si-FH, and lepidocrocite (LEP) at pH 7.0 in 24 hours. Initial conditions: 50 μM FMN or RBF, 30 mM Fe(III) oxide.

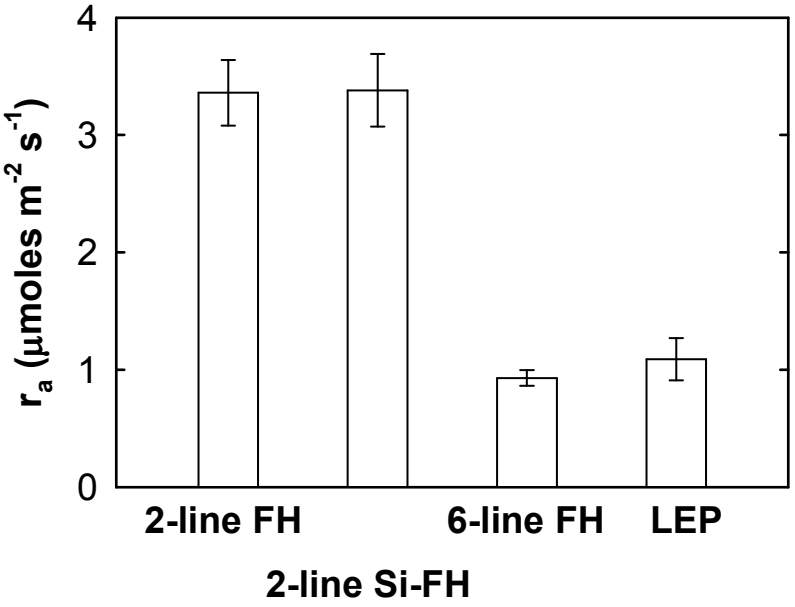

Figure S9. Surface area normalized initial reaction rate (r_a) of reactions shown in Figure 3(a) in the main text. Error bars represent one standard deviation from 6 experiments with 10 μM - 200 μM iron oxide concentrations.